[Downloaded from www.aece.ro on Friday, March 29, 2024 at 01:45:36 (UTC) by 44.200.74.73. Redistribution subject to AECE license or copyright.]

Variable Structure Control of DFIG for Wind Power Generation and Harmonic Current Mitigation

Djilali KAIRUS[1,3], René WAMKEUE[2], Bachir BELMADANI[1], Mustapha BENGHANEM[3]
[1]*Chlef University UHBC, Chlef, 02000, Algeria*
[2]*University of Québec in Abitibi-Témiscamingue (UQAT) Québec (QC), J9X 5E4, Canada*
[3]*Electrical Engineering Faculty, USTO-MB, Oran 31000, Algeria*
kdjilali@hotmail.com

***Abstract*—This paper focuses on wind energy conversion system (WECS) analysis and control for power generation along with problems related to the mitigation of harmonic pollution in the grid using a variable-speed structure control of the doubly fed induction generator (DFIG). A control approach based on the so-called sliding mode control (SMC) that is both efficient and suitable is used for power generation control and harmonic-current compensation. The WECS then behaves as an active power filter (APF). The method aims at improving the overall efficiency, dynamic performance and robustness of the wind power generation system. Simulation results obtained on a 20-kW, 380-V, 50-Hz DFIG confirm the effectiveness of the proposed approach.**

***Index Terms*—Active filter, Doubly Fed Induction Generator, Power Quality, SMC, Power Quality.**

I. INTRODUCTION

Due to its flexibility, stability and the fact that the associated power electronic converter requires only a fraction of the total power, the wind energy conversion system (WECS) using a DFIG has become very popular for variable-speed wind turbine generation [1]-[3]. In previous papers [1]-[3], different DFIG vector control schemes have been developed. In [1], the stator flux control of the DFIG using conventional PI regulators is presented, while in [2] and [3] direct torque control of the DFIG is outlined.

However, the DFIG has to endure two types of interference during system operation: (a) external interference, which refers to load torque oscillations on the driving chain due to random variation of the wind speed and direction; (b) internal interference, which refers to the mismatch of controllers and machine parameters caused by changes in the generator temperature, magnetic saturation level and skin effect [4]. These two kinds of interference affect the working efficiency, dynamic performance, and robustness of the wind power generation system. In such circumstances, conventional controllers based on PI-regulators cannot follow the changes in system parameters and are thus useless.

Meanwhile, grids now have to deal with increasing harmonic pollution due to nonlinear loads such as power electronics converters and large AC drives, with the result that power quality has become a major challenge in integrating WECS into electrical grids. A few research groups have addressed the possibility of making use of built-in WECS converters to improve grid power quality and achieve harmonic-current mitigation [5], [6].

More recently, the active power filter (APF) for wind turbines with synchronous generator has been studied [7] while in [8] a variable-speed WECS with a high-selectivity harmonic filter has been developed.

An efficient and more suitable control approach based on sliding-mode control (SMC) is proposed in this paper for simultaneous power generation control and harmonic-current mitigation. The SMC is a kind of nonlinear control method based on a state space model of a DFIG [9]. Control characteristics of the SMC could force the controlled variables to move along the scheduled track. Compared to PI control, the proposed approach offers a faster response and characteristics insensitive to parameter variation and interference [10], [11].

The paper is organized as follows: section II presents the entire system under study. The state modelling, control strategy and design of the SMC approach are dealt with in section III while section IV focuses on harmonic compensation. In section V, results of simulations to validate the proposed DFIG control framework are presented and discussed. Finally, section VI concludes the study and announces future steps in our work presented in this paper.

II. DESCRIPTION AND MODELING OF THE SYSTEM

The basic configuration of the whole system is presented in Fig.1. The rotor of the DFIG is connected to the grid through two back-to-back bridge converters. The PWM grid-side converter (GSC) is used to control the DC-link voltage and keep it constant regardless of the magnitude and direction of the rotor power. The PWM rotor side converter (RSC) is used to generate the optimal active power depending on the wind speed and turbine characteristics. The SMC can be modified in the rotor side converter taking into account the active filtering function. In this case, the RSC will take on the role of an active parallel filter (APF) and is required in order to mitigate the harmonic pollution. The particularity of this system, therefore, is its ability to simultaneously capture maximum energy from the wind fluctuation, control the active and reactive power and compensate the grid harmonic currents. The transformer is

Digital Object Identifier 10.4316/AECE.2010.04027

1582-7445 © 2010 AECE

[Downloaded from www.aece.ro on Friday, March 29, 2024 at 01:45:36 (UTC) by 44.200.74.73. Redistribution subject to AECE license or copyright.]

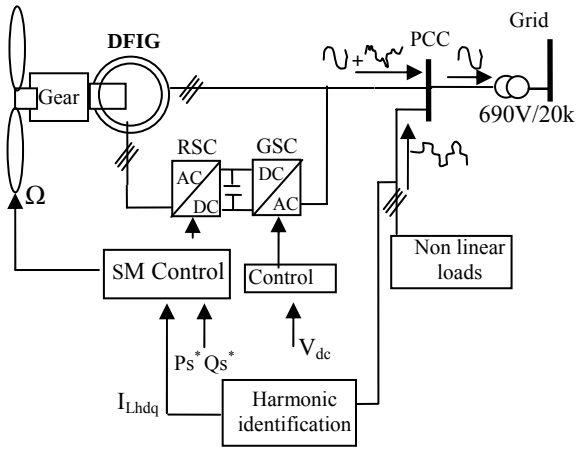

Fig. 1. Schematic representation of DFIG-based wind turbine

considered to be linear (magnetic saturation is not taken into account in the study). Also, it is assumed that the average PWM back-to-back converters have no losses. The rotor side converter (RSC) model reproduces the reference voltages generated by the control scheme.

The electrical equations of the wound-rotor induction machine in the d-q reference frame are as follows [12]:

$$V_{dqs} = R_s I_{dqs} + \frac{d\varphi_{dqs}}{dt} + \Xi\ \omega_s \varphi_{qds} \tag{1}$$

$$V_{dqr} = R_r I_{dqr} + \frac{d\varphi_{dqr}}{dt} + \Xi\ \omega_r \varphi_{qdr} \tag{2}$$

With:

$$\varphi_{dqs} = L_s I_{dqs} + M I_{dqr} \tag{3}$$

$$\varphi_{dqr} = L_r I_{dqr} + M I_{dqs} \tag{4}$$

$$\Xi = \begin{bmatrix} 0 & -1 \\ 1 & 0 \end{bmatrix} \tag{5}$$

Subscripts *d* and *q* refer to the d- and q-axes respectively and subscripts *s* and *r* to the stator and rotor of the DFIG respectively; ω_s and ω_r (in rad/s) are the stator and rotor variable pulsations respectively; V_{dq}, I_{dq} and φ_{dq} are voltage current and flux vectors respectively in the d-q reference frame; R_s and R_r are stator and rotor resistances; L_s and L_r are the stator and the rotor leakage inductance and M is the magnetizing inductance. Ξ is the coupling-axes matrix The electromechanical equation is expressed by:

$$J\frac{d\Omega}{dt} + f_0\Omega = T_e - T_r \tag{6}$$

$$T_e = p\left(\varphi_{ds} I_{qs} - \varphi_{qs} I_{ds}\right) \tag{7}$$

Where p is the number of the pole pair, T_r mechanical torque, T_e electrical torque, J the inertia constant, Ω rotor speed, and f_0 is the friction coefficient.

III. CONTROL STRATEGY OF THE DFIG

A. Decoupling of the active and reactive powers

In an aim to decouple the active and reactive power, the stator flux vector will be aligned with the q-axis. So, by neglecting the stator resistance and assuming that the stator flux φ_{ds} is maintained constant, we then have:

$$\begin{cases} V_{ds} = 0 \\ V_{qs} \approx \omega_s \varphi_{ds} = V_s \end{cases} \tag{8}$$

From equations (3) and (4), the stator currents and rotor flux can be written as:

$$I_{ds} = -\frac{M}{L_s} I_{dr} + \frac{\varphi_s}{L_s} \tag{9}$$

$$I_{qs} = -\frac{M}{L_s} I_{qr} \tag{10}$$

$$\varphi_{dr} = \delta L_r\ I_{dr} + \frac{M\ \varphi_s}{L_s} \tag{11}$$

$$\varphi_{qr} = \delta L_r\ I_{qr} \tag{12}$$

δ is the Blondel dispersion coefficient, defined as:

$$\delta = \left(1 - \frac{M^2}{L_s L_r}\right) \tag{13}$$

By substituting the equations (11) and (12) in (2), the rotor voltage equations become:

$$V_{dr} = R_r I_{dr} + \delta L_r \frac{d I_{dr}}{d t} - g_{ls}\omega_s L_r \delta\ I_{qr} \tag{14}$$

$$V_{qr} = R_r I_{qr} + \delta L_r \frac{d I_{qr}}{d t} + g_{ls}\omega_s L_r \delta I_{dr} + g_{ls}\omega_s \frac{M\varphi_s}{L_s} \tag{15}$$

From equations (14) and (15) it is observed that the desired rotor currents I_{dr} and I_{qr} can be fixed by the rotor voltages V_{dr} and V_{qr} respectively. The coupling term δL_r can be compensated in the control strategy. The term $g_{ls}\omega_s \frac{M\varphi_s}{L_s}$ represents the electromotive force. Consequently, the two rotor current components I_{dr} and I_{qr} are decoupled. The active and reactive power can therefore be controlled separately from the rotor reference currents. The torque, the stator active and reactive powers are expressed by:

$$T_e = P\frac{M}{L_s}\varphi_s\ I_{qr} \tag{16}$$

$$P_s = (V_{ds} I_{ds} + V_{qs}.I_{qs}) = -\varphi_s\ \omega_s\ I_{qr}\frac{M}{L_s} \tag{17}$$

$$Q_s = (V_{qs} V_{ds} - V_{ds}.I_{qs}) = \frac{\varphi_s^2}{L_s}\omega_s - \frac{M}{L_S}\varphi_s \omega_s\ I_{dr} \tag{18}$$

Equations (17) and (18) show that the rotor reference currents can be derived from stator power references; thus,

[Downloaded from www.aece.ro on Friday, March 29, 2024 at 01:45:36 (UTC) by 44.200.74.73. Redistribution subject to AECE license or copyright.]

the analysis of DFIG in the $d-q$ system yields the following properties (summarized in Table1).
The previous system equations can be organized in the state form (19) which will be used to design the SMC power controllers.

TABLE I. DIFFERENT MODE PROPERTIES OF DFIG CONTROLS

Control of	**Function with**
Speed (tr/mn)	$N = f\ (g_{ls})$
Electromagnetic Torque	$T_e = f\ (I_{qr})$
Stator Active Power	$P_s = f\ (I_{qr})$
Stator Reactive Power	$Q_s = f\ (I_{dr})$

$$\dot{x} = f(x,t) + g(x,t)\,U \tag{19}$$

With:

$$U = \begin{bmatrix} V_{ds} & V_{qs} & V_{dr} & V_{qr} \end{bmatrix} \tag{20}$$

$$\dot{x} = \begin{bmatrix} \frac{d\varphi_{ds}}{dt} & \frac{d\varphi_{qs}}{dt} & \frac{d\varphi_{dr}}{dt} & \frac{d\varphi_{qr}}{dt} \end{bmatrix}^T \tag{21}$$

$$g(x,t) = \begin{bmatrix} 1 & 0 & 0 & 0 \\ 0 & 1 & 0 & 0 \\ 0 & 0 & \frac{1}{\sigma L_r} & 0 \\ 0 & 0 & 0 & \frac{1}{\sigma L_r} \end{bmatrix} \tag{22}$$

$$f(x,t) = \begin{bmatrix} f_{11} & f_{12} \\ f_{21} & f_{22} \end{bmatrix} \tag{23}$$

$$\begin{cases} f_{11} = -a\ R_s \varphi_{ds} - R_s c \left(L_r \delta I_{dr} + \dfrac{M}{\omega_s L s} V_{qs} \right) + \omega_s \varphi_{qs} \\ f_{12} = -a\ R_s \varphi_{qs} - R_s c \left(L_r \delta I_{qr} + \dfrac{M}{\omega_s L s} V_{ds} \right) - \omega_s \varphi_{ds} \\ f_{21} = \dfrac{1}{\delta L_r} - \left(bR_r \left(L_r \delta I_{qr} + \dfrac{M}{\omega_s L s} V_{qs} \right) \right) \\ \qquad \cdots + cR_r \varphi_{ds} + \omega_s \left(L_r \delta I_{qr} + \dfrac{M}{\omega_s L s} V_{ds} \right) \\ f_{22} = \dfrac{1}{\delta L_r} - \left(bR_r \left(L_r \delta I_{qr} + \dfrac{M}{\omega_s L s} V_{qs} \right) \right) \\ \qquad \cdots + cR_r \varphi_{ds} + \omega_r \left(L_r \delta I_{dr} + \dfrac{M}{\omega_s L s} V_{qs} \right) \end{cases} \tag{24}$$

$$a = \frac{1}{\sigma L_s}, b = \frac{1}{\sigma L_r}, c = \frac{M}{\sigma L_s L_r} \tag{25}$$

B. Design sliding mode control (SMC)

SMC is basically an adaptive technique whose output variable is forced to track the desired response. It offers several advantages, such as robustness, good dynamic response and simple implementation. In addition, it involves an important aspect related to the stability even for large supply load variations, where the power system stability has been recognized as an important problem for secure system operation [5].

Many papers have been proposed for controlling WECSs with DFIG [1],[2]-[13] but, in many of these studies, the system stability analysis is not included. In contrast to classical control methods using PI controllers, ensuring system stability after severe network disturbances is one of the main advantages of the SMC developed in this paper. [14].

The basis of the SMC theory is the specification of a sliding surface: the surface is chosen such that the control features will keep the system within the surface and, hence, follow the desired system behavior. The objective of this control technique is to determine the parameters of each structure together with the commutation functions. Switching from one structure to another makes it possible to reap the benefits of each structure.

In general, four basic steps are required when designing the SMC: a) selection of a sliding surface; b) design of a test to verify the sliding-mode existence; c) stability analysis within the surface; d) determination of the control input U_n with the objective that every state outside the commutation surface should be joined in a finite time. Thus, the system will take on the dynamics of the selected surface and move on to the point of equilibrium.

The desired control vectors force the trajectory of the system to converge towards the surface defined by:

$$\sigma_{dq}(x) = 0 \tag{26}$$

In order to control the output current of the inverter, a suitable sliding surface is chosen, which is directly affected by the switching law. This sliding surface is chosen in general as hyper plants through the origin of space. We define the sliding surface in the Park reference as follows:

$$\sigma_{dq}(x) = \lambda (I_{dqr\_ref} - I_{dqr}) \tag{27}$$

where I_{dqr_ref} and I_{dqr_mes} are the reference and the measured rotor current vectors respectively. The choice of parameter λ guarantees the stability of the system at a given time. In order to guarantee the attraction of the system throughout the surface (guaranteeing the sliding mode's existence), the following condition must be fulfilled:

$$\dot{\sigma}_{dq}\ \sigma_{dq} < 0 \tag{28}$$

The equivalent command (in (19)) corresponding to the ideal sliding regime is obtained by imposing: $\dot{\sigma}_{dq}(x) = 0$

$$\dot{\sigma}_{dq}(x,t) = \left(\frac{\partial \sigma}{\partial x} \right)^T \frac{\partial x}{\partial t} = \left(\frac{\partial \sigma}{\partial x} \right)^T \left(f(x,t) + g(x,t)\,U_{eq} \right) \tag{29}$$

From (23) we have:

[Downloaded from www.aece.ro on Friday, March 29, 2024 at 01:45:36 (UTC) by 44.200.74.73. Redistribution subject to AECE license or copyright.]

$$U_{eq} = -f(x,t)\left(\frac{\partial\sigma}{\partial x}\right)^{T}\left[\left(\frac{\partial\sigma}{\partial x}\right)g(x,t)\right]^{-1} \quad (30)$$

with the condition of the existence of the sliding mode:

$$\left[\left(\frac{\partial\sigma}{\partial x}\right)g(x,t)\right]^{-1} \neq 0 \quad (31)$$

Equation (25), showing the boundary conditions, implies that the field vector g is not orthogonal to the normal vector of the surface, so *g* has no component vertical to the surface σ and the state of the system cannot return to this surface

With $\dot{\sigma}_{dq}(x) = 0$, the equivalent control vector U_{eq} can be expressed by:

$$U_{eq} = \begin{bmatrix} -\left(\begin{array}{l} -R_r b\left(L_r\sigma I_{dr} + \dfrac{M}{L_s\omega_s}V_{qs}\right) \\ +R_r\, c\,\varphi_{ds} + \omega_r\left(L_r\sigma I_{qr} + \dfrac{M}{L_s\omega_s}V_{ds}\right)\end{array}\right) \\ -\left(\begin{array}{l} R_r b\left(L_r\sigma I_{qr} + \dfrac{M}{L_s\omega_s}V_{ds}\right) \\ +R_r\, c\,\varphi_{qs} + \omega_r\left(L_r\sigma I_{dr} + \dfrac{M}{L_s\omega_s}V_{qs}\right)\end{array}\right) \end{bmatrix} \quad (32)$$

In order to obtain good dynamic performances and commutation around the surface, the control vector is modified as shown below:

$$U = U_{eq} - U_n \quad (33)$$

U_n is the Signum function defined by:

$$U_n = -K\ sign(\sigma_{dq}) \quad (34)$$

U_{eq} is valid only for the sliding surface and U_n ensures the sliding mode's existence. The DFIG global sliding-mode control is illustrated in detail in Fig.2.

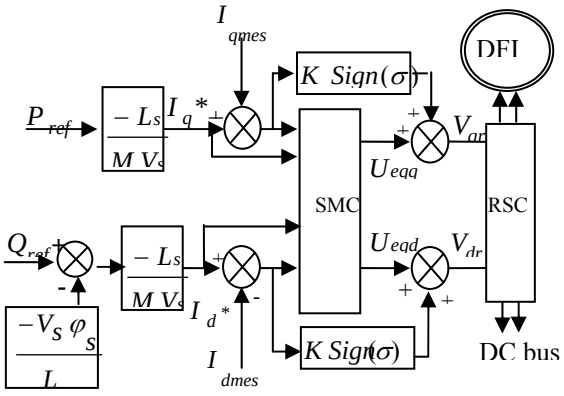

Fig. 2. General diagram of simulation and control of DFIG by the SMC

IV. MODIFIED RSC CONTROL FOR HARMONIC COMPENSATION

The power active filter (PAF) technology is now mature enough to provide compensation for harmonics, reactive power, and/or the neutral current in AC networks. It has evolved in the past quarter century of development with varying configurations, control strategies, and solid-state devices. PAFs are also used to eliminate voltage harmonics, regulate terminal voltage suppress voltage flicker and improve voltage balance in three-phase systems [16]. This wide range of objectives is achieved either individually or in combination, depending on the requirements as well as the control strategy and configuration, which have to be selected appropriately. This section describes the ability of the DFIG to have exactly the same behaviour as an APF.

A. Harmonic compensation

The presence of nonlinear loads on the grid is accompanied by the generation of pulling currents (Fig 1). The current supplied by the grid is defined by:

$$I_N = I_{gr} - I_L \quad (35)$$

I_{gr}, I_g, I_L are the grid, the generator and the load currents respectively. The load current I_L can be organized as follows:

$$I_L = I_{Lf} + I_{Lh} \quad (36)$$

I_{Lh}, I_{Lf} are the harmonic and the fundamental currents. In order to ensure good power quality without any distortion (a sinusoidal grid current), the RSC is used as an active parallel filter (APF) and, as such, it provides harmonic currents with an equal magnitude load harmonic current I_{Lh} and opposite phase.

B. Harmonic identification

Good harmonic identification is required to have good compensation. Thus, in order to obtain the desired compensation signals, three steps are indispensable: 1) appropriate dimensioning of APF devices, 2) appropriate selection of the harmonic identification algorithm, and 3) appropriate design of the control unit allowing generation of the switching orders.

A time-domain harmonic detection method is used for harmonics isolation (Fig. 3). This technique, applied in an APF for the first time by Akagi [17] and known as the 'instantaneous power p–q theory', consists in extracting harmonics from the load currents by the computation of instantaneous power p–q in the $\alpha\beta$ reference.

The transformation of the currents $abc / \alpha\beta$ is given by:

$$\begin{bmatrix} I_\alpha \\ I_\beta \end{bmatrix} = \sqrt{\frac{2}{3}}\begin{bmatrix} 1 & -0.5 & -0.5 \\ 0 & \dfrac{\sqrt{3}}{2} & -\dfrac{\sqrt{3}}{2} \end{bmatrix}\begin{bmatrix} I_a \\ I_b \\ I_c \end{bmatrix} \quad (37)$$

where, the voltages have a similar transformation. In the reference $\alpha\beta$, the instantaneous powers are defined by:

$$\begin{bmatrix} P \\ Q \end{bmatrix} = \begin{bmatrix} V_\alpha & V_\beta \\ -V_\beta & V_\alpha \end{bmatrix}\begin{bmatrix} I_\alpha \\ I_\beta \end{bmatrix} \quad (38)$$

Decomposition of the active and reactive powers gives continuous and alternative components:

$$P = \bar{P} + \tilde{P} \quad (39)$$

[Downloaded from www.aece.ro on Friday, March 29, 2024 at 01:45:36 (UTC) by 44.200.74.73. Redistribution subject to AECE license or copyright.]

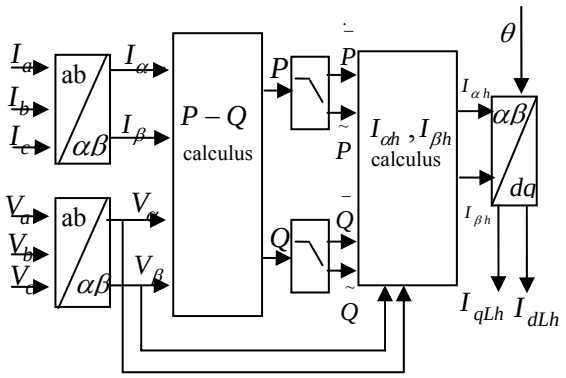

Fig. 3. Diagram of the p-q instantaneous powers theory

$$Q = \bar{Q} + \tilde{Q} \tag{40}$$

$\bar{P}$, $\bar{Q}$: continuous components

$\tilde{P}$, $\tilde{Q}$: sum of the harmonics components

C. Modified RSC control

The rotor currents corresponding to the powers without harmonic compensation are given by equations (41) and (42) while the harmonic currents associated with the pollutant load are defined by (43) and (44).

$$I_{dr} = \frac{\varphi_s}{M} - \frac{L_s}{M} I_{ds} \tag{41}$$

$$I_{qr} = -\frac{L_s}{M} I_{qs} \tag{42}$$

$$I_{drh} = -\frac{L_S}{M} I_{dLh} \tag{43}$$

$$I_{qrh} = -\frac{L_S}{M} I_{qLh} \tag{44}$$

The new current references that follow the power reference without harmonics in the grid are given by:

$$I_{drt} = I_{drh} + I_{dr} \tag{45}$$

$$I_{qrt} = I_{qrh} + I_{qr} \tag{46}$$

Equations (39) and (40) present the superposition of two currents in each axis. The SMC produces the corresponding reference voltages generated by the rotor side converter.

V. SIMULATION RESULTS

To demonstrate the pertinence of the proposed DFIG sliding-control approach, simulations have been performed using MATLAB/ SIMULINK software on a 20-kW, 380-V, 50-Hz wound-rotor induction machine with the following parameters:

$M = 0.034H$, $Rs = 0.0455\Omega$, $Rr = 0.19\Omega$, $Ls = 0.07H$,

$Lr = 0.0213H$ $f_0 = 0.0024$, $Js = 0.53 kg.m^2$

A. Dynamic behaviour of the DFIG

a) First, the power reference values are changed at t=1s from -10 kW to -15 kW for the active power (Fig. 4a), and at t=2s from -5 kVA to 0 kVA for the reactive power (Fig. 4c).The simulation results show the step change of the rotor q-axis current at t=0.8s (Fig. 4b) while the step change of the d-axis current occurs at t=1s (Fig.4d). The decoupled d-q rotor currents guarantee the decoupled active and reactive powers, as previously announced in section IV.

b) In the second stage, a voltage dip fault that is 50% lower than the rated value is produced at t=3.5s followed, after 300 ms, by a fault clearance at t=3.7s. Figures 4a-4h show the transient behavior of powers, currents, torque, and speed during the voltage dip. Voltage dips are generally due to short circuits somewhere in the grid, switching operations associated with temporary disconnection of a supply and the flow of large currents during the start-up of large motors. Figures 4e and 4f show transient states during a voltage dip of the electromagnetic torque and the speed respectively, while Figs.4g and 4h illustrate the stator and rotor currents respectively.

It was found that, during an AC voltage dip, the most critical situation, when both rotor speed and stator active power output were at their maximum values prior to the AC fault, a high rotor speed value generates a higher peak voltage on the rotor side of DFIG.

A large-magnitude voltage from the converter is required for adequate control during an AC voltage dip but,

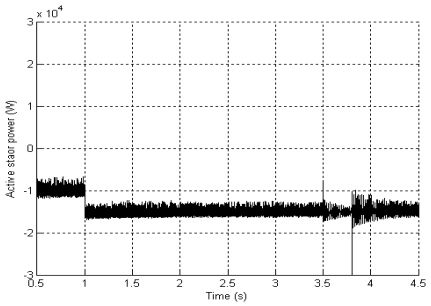

a. Active power

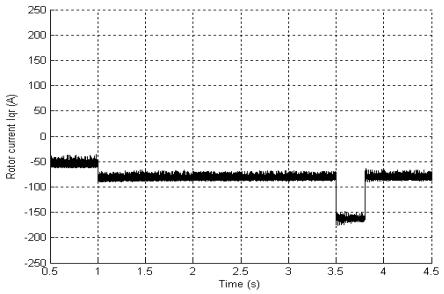

b. Rotor current

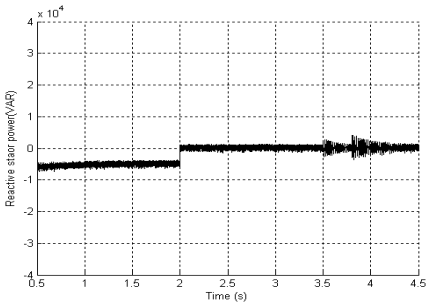

c. Reactive power

[Downloaded from www.aece.ro on Friday, March 29, 2024 at 01:45:36 (UTC) by 44.200.74.73. Redistribution subject to AECE license or copyright.]

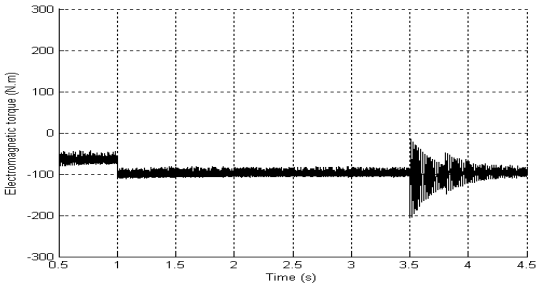

d. Rotor current I_{dr}

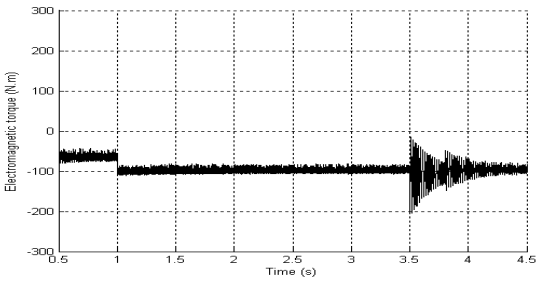

e. Electromagnetic torque

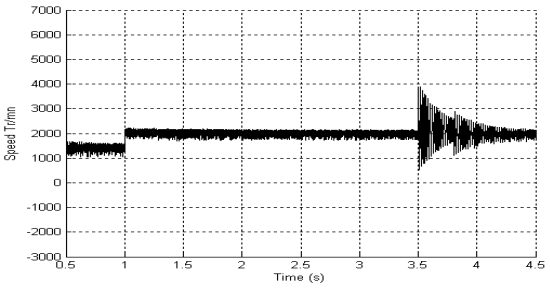

f. Speed

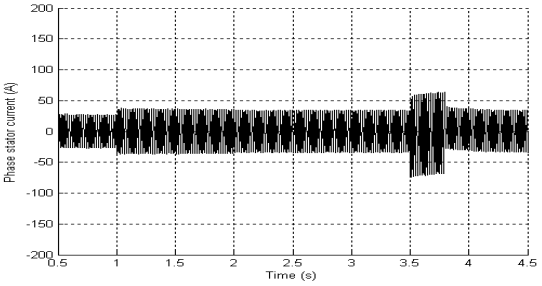

g. Phase stator current

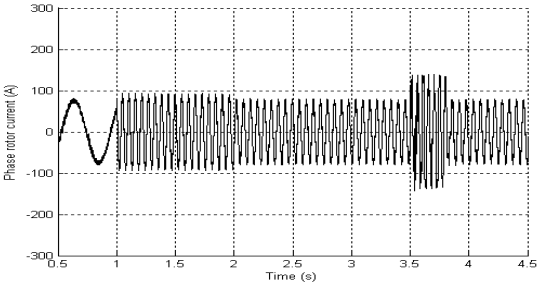

h. Phase rotor current

Fig. 4. Dynamic behaviour of DFIG with SMC during a voltage dip

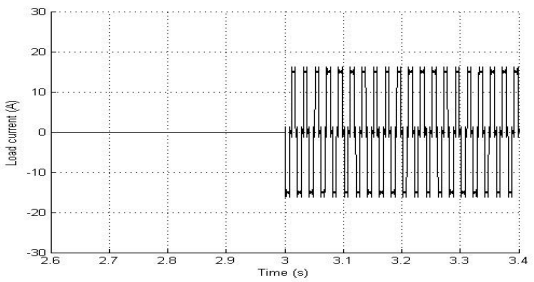

Fig. 5. Load current

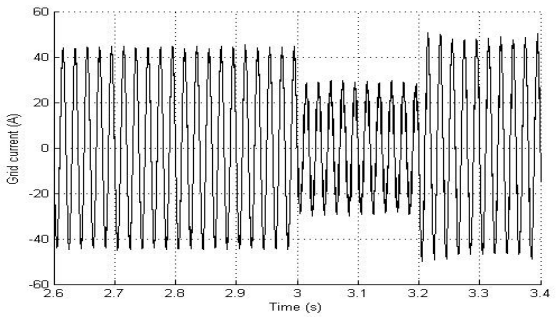

Fig. 6. Grid current during connection of the polluting load and APF

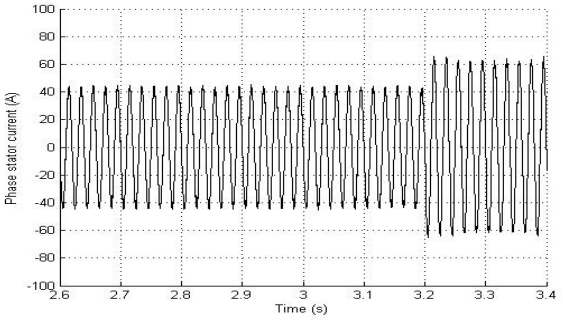

Fig. 7. Stator current during connection of the polluting load and APF

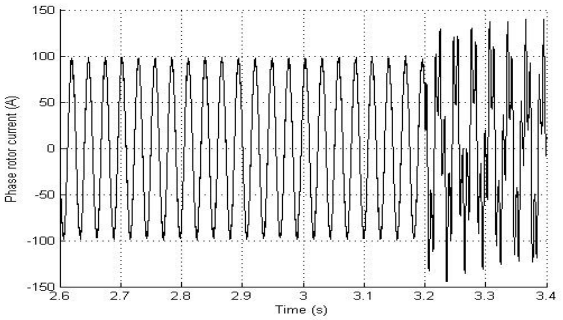

Fig. 8. Rotor current during connection of the polluting load and APF

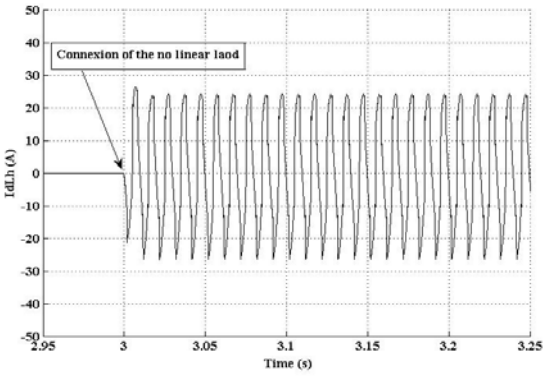

a. Load harmonic current reference for the harmonic compensation

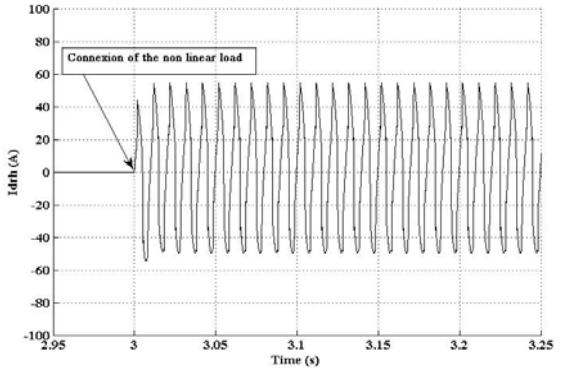

b. Load harmonic current reference reported on the rotor

[Downloaded from www.aece.ro on Friday, March 29, 2024 at 01:45:36 (UTC) by 44.200.74.73. Redistribution subject to AECE license or copyright.]

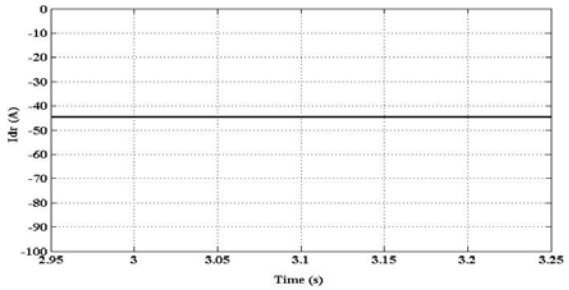

c.Rotor current reference for the power.

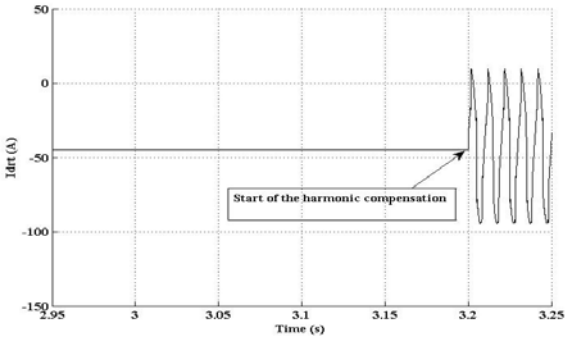

d.Total rotor current reference.

Fig. 9. *d*-axis current references

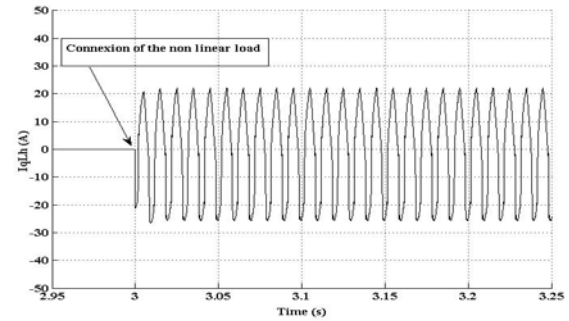

a. Load harmonic current reference for compensation

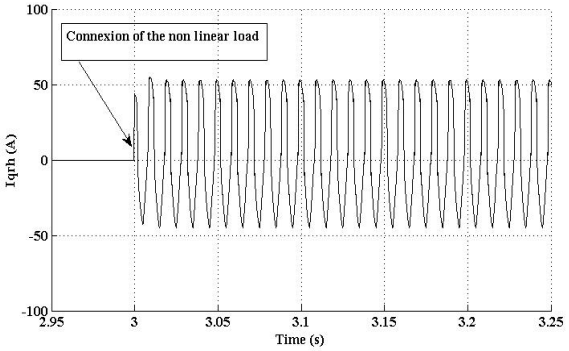

b.Load harmonic current reference reported on the rotor

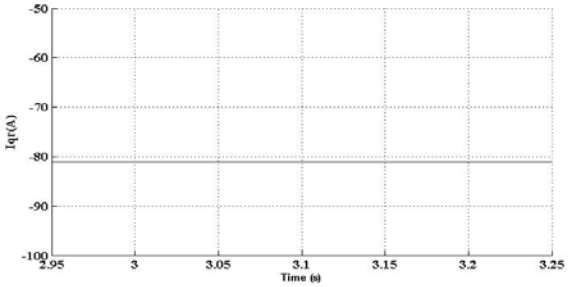

c.Rotor current reference for the power

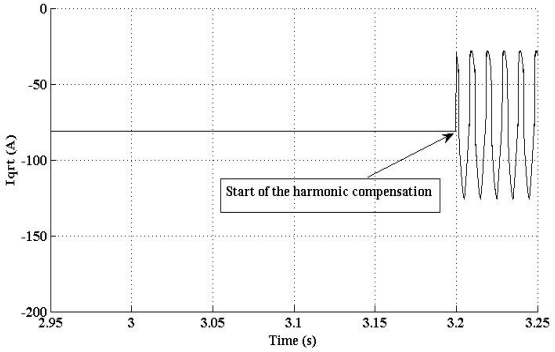

c- Total reference rotor current command.

Fig. 10. *q*-axis current references

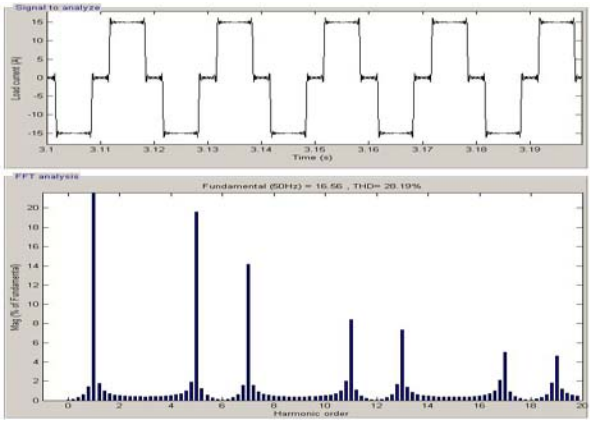

Fig. 11. FFT and Zoom on load currents.

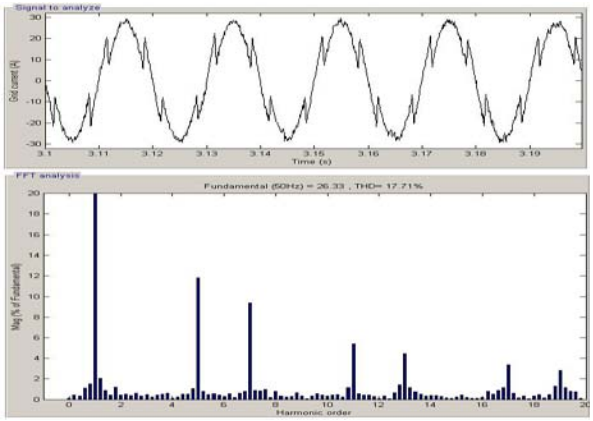

Fig. 12. Zoom on grid currents and FFT after connection of polluting load without control.

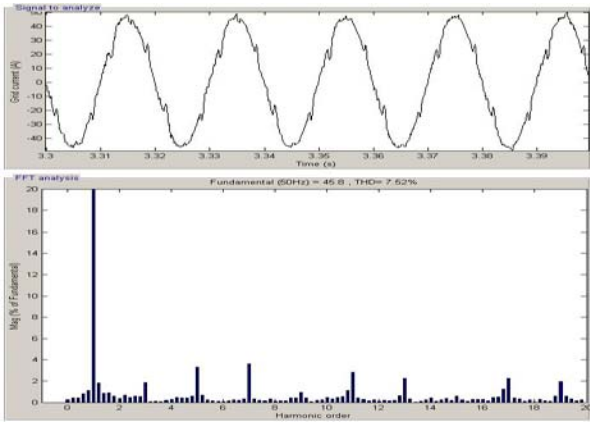

Fig. 13. Zoom on grid currents and FFT after connection of polluting load with APF control.

[Downloaded from www.aece.ro on Friday, March 29, 2024 at 01:45:36 (UTC) by 44.200.74.73. Redistribution subject to AECE license or copyright.]

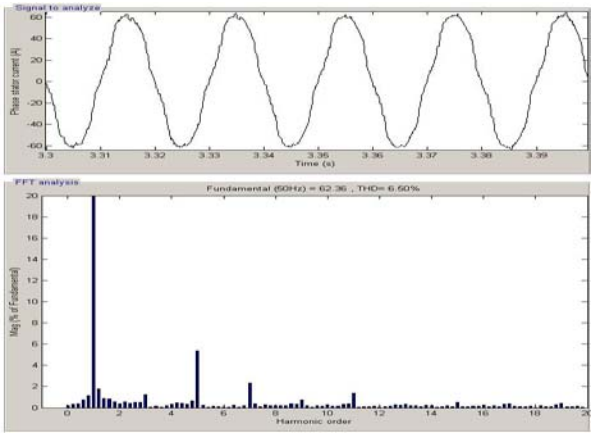

Fig. 14. Zoom on stator current and FFT after connection of polluting load with APF control.

unfortunately, only a limited voltage can be generated by the converter. In addition, the clearance time has a great effect on the FRT capability of the WECS. System stability is maintained during voltage dips. The SMC makes a good contribution in this way. Without the voltage limit, the voltage dip can cause a high stator current (Fig.4e) and, hence, a high induced voltage and current in the rotor circuit (Fig.4h). which could destroy the converter if nothing is done to protect it.

In the literature, authors have proposed connecting an additional resistance to the rotor, called a "crowbar". At the moment of the fault occurrence, the crowbar connected to the rotor and the rotor-side converter must be disconnected. The problem with this protection system is that it can be applied only for symmetrical faults; in addition a highly reactive power will be absorbed by the DFIG, resulting in grid disturbances.

B. Active filtering

For this simulation, the voltage is kept constant. A polluting load is connected at t=3 s (Fig.5), while the active filter control turns on at t=3.2 s. Figures 6, 7 and 8 illustrate the behaviour of the grid, stator and rotor currents, respectively, while Figs.9 and 10 show the harmonic references (according to the *d*- and *q*-axis respectively) identified and injected into the rotor side converter.

The total load harmonic distortion (THD) = 28.19% is shown in Fig.11. With this polluting load, the grid current has a THD=17.5% (Fig.11).

This pollution causes a distortion signal for other users connected to the PCC. The active filtering capability of the DFIG can reduce these harmonics (by modifying the SMC). Using the THD calculation, the THD of the grid current is improved from 17.5% to 7.5% (Figs. 12 and 13). However, Fig.14 shows the DFIG current (I_g) in this active filtering case with THD=6.5%.

A dilemma arises between the value to be compensated and the value of the total harmonics produced by the generator. However, high harmonics in the rotor and the stator of the DFIG will have a large effect on the general performance and life duration of DFIG.

VI. CONCLUSION

The focus of this paper has been on the SMC as a means of ensuring high DFIG dynamic performances. A novel approach is proposed for improving the power quality of the grid using a WECS based on a DFIG. The paper also describes an attempt to improve DFIG control in order to achieve active and reactive green power sources along with an active filtering capability.

Simulation results clearly attest to the effectiveness of the DFIG sliding control and filtering framework analysis. However, it has been shown that high-frequency currents are injected on the rotor and stator sides of the DFIG. This appears to be a real problem for full harmonic compensation of the system. For future work, after validation of the present paper with actual data, it is planned to thoroughly explore reliable solutions for harmonic current injection following application of the proposed SMC control approach.

REFERENCES

[1] R. Pena, R.C. Clark, G.M. Asher, Doubly Fed Induction Generator using Back-to-Back PWM Converters and its Application to Variable-Speed Wind-Energy generation, IEE Proc-Elect. Power Appl, Vol. 143, N°5.1969. pp. 380-387.

[2] Lie Xu P. Cartwright, Direct Active and Reactive Power Control of DFIG for Wind Energy Generation, IEEE Transactions on Energy Conversion. 21, No. 3, Sept. 2006. pp. 750–758.

[3] D. Zhi and L. Xu, Direct Power Control of DFIG with Constant Switching Frequency and Improved Transient Performance, IEEE Trans. on Energy Conversion, Vol. 22, N°. 1, March 2007, pp. 110-118.

[4] X. Xiaozeng, L. Yezeng, and Q. Yin, Effect of Parameters Variety on Vector-Controlled Induction Motor, J. Huazhong Univ. of Sci. & Tech. (Nature Science Edition), Vol.30, N° 7, 2003 pp. 43-45.

[5] V. Utkin, Va riable Structure Systems with Sliding Mode, IEEE.Trans. Automatic Control, 22(2). 1997. Pp.212-222.

[6] V.I. Utkin, Sliding Mode Control Design Principles and Applications to Electrical Drives, IEEE Trans. On industrial Electronics, Vol. 40, N° 1, Feb. 1993, pp. 41-49.

[7] T.S. Key and 1.-S. Lai, Comparison of Standards and Power Supply Design Options for Limiting Harmonic Distortion in Power Systems Update, IEEE Trans. Ind. Appl., Vol. 29, N°. 4, July/Aug. 1993. pp. 688-695.

[8] K.J.P. Macken, K. Vanthournout, J. Van den Keybus, G. Deconinck , R.J.M. Belmans, Distributed Control of Renewable Generation Units with Integrated Active Filter, IEEE Transactions on Power Electronics, Vol.19. Sept. 2004. pp. 1353–1360.

[9] M.T. Abolhassani, P. Enjeti, H.A. Toliyat, Integrated Doubly-Fed Electric Alternator/Active Filter (IDEA), a Viable Power Quality Solution, for Wind Energy Conversion Systems, IEEE Trans. Energy Conversion, Vol. 23, N° 2, June 2008, pp. 642-650.

[10] F. Soares dos Reis, J.A.V. Alé, F. D. Adegas, R.Tonkoski Jr, S.Slan, K. Tan, Active Shunt Filter for Harmonic Mitigation in Wind Turbines Generators, 37th IEEE. Power Specialists Conference, Jeju, Korea. June 18-22, 2006.

[11] A. Gaillard, P. Poure, S. Saadate, M. Machmoum, Variable Speed DFIG Wind Energy System for Power Generation and Harmonic Current Mitigation, Renewable Energy.34, 2009, pp.1545-1553

[12] P.C. Krause, Analysis of Electrical Machinery, New York, McGraw-Hill. 1994.

[13] L. Mihet-popa, I. BOLDEA, Control Strategies for Large Wind Turbine Application, Journal of Electrical Engineering, Vol. 7, Edition 3rd, ISSN 1582-4594. 2006.

[14] K.Y. Chang, W.J. Wang, Robust Covariance Control for Perturbed Stochastic Multivariable System via Variable Structure control", Elsevier, Systems & Control Letters 37 (1999) pp.323-328.

[15] M. Hamerlain, T. Youssef, M. Belhocine, Switching on the derivative of control to reduce chatter, IEE Proceeding Control Theory and Applications, Vol.148, Issue 1, Jan 2001.

[16] B. Singh, K. Al-Haddad, A. Chandra, A Review of Active Filters for Power Quality Improvement, IEEE Trans. on Ind. Electronics, Vol. 46, N°. 5, October 1999. pp 960-971.

[17] A. Akagi, Y. Kanazawa and A. Nabae, Instantaneous Reactive Power Compensation comprising Switching Devices Without Energy Storage Elements, IEEE Trans. on Ind. App. Vol. 20, 1984.